Right-Angled V-Shaped conformal Dual-Patch Antenna Array for RAIN RFID Doorway Portals

Dr. Prabakar Parthiban, *Graduate Member, IEEE*.

***Abstract*— This paper presents a conformal ultra-high-frequency (UHF) radio frequency identification (RFID) reader antenna array for doorway portal applications. The dual-patch antenna is only 100 mm wide and right-angled (V-shaped) to fit the corners of a regular portal. Patches are arranged orthogonally to create horizontal and vertical-linearly polarized fields at near-zones and at far-field distances they provide slant-polarized fields. Beam steering is enabled by phase delaying the array elements to enhance the field coverage within the doorway portal. The antenna operates in the European UHF RFID band (865-868 MHz) with a 38 MHz, 10 dB impedance bandwidth. The antenna's azimuth and elevation half-power beamwidth is 90° and 130°. The azimuth beam is tilted to 35° from the boresight where the gain is peaked at 5.5 dBi. This antenna is low-profile, low-cost and flame retardant and paintable. Inherited properties of the antenna's substrate make the antenna non-toxic, self-extinguishing, lightweight and highly chemical resistant. The reader antenna is compatible with both RAIN and non-RAIN alliance UHF RFID readers.**

***Index Terms*— UHF RFID; right-angled antenna; L-Shaped; V-Shaped patch antenna; portal antenna; door frame.**

I. Introduction

RAIN (RAdio frequency IdentificatioN) is a technology alliance that promotes global adoption of UHF (Ultra-High Frequency) RFID (Radiofrequency Identification) utilizing the GS1 Gen2 standards in accordance with the ISO/IEC 18000-63. RAIN RFID system consists of items, tags, reader and antennas, software and network [1]. RAIN RFID system is typically used to identify, locate, authenticate and engage with items/assets. A portal/doorway application is one of the commonly used applications to track assets going through an entranceway.

Various types of assets, right from cartons of a variety of goods or people with lanyard badges or loose handheld assets such as folders, traverse through a doorway/portal. There are a lot of factors that hinder reliable tag detection. Assets may bear tag in any orientation, and thus it is crucial to create diversified RF fields for efficient detection. As most of the tag antenna designs are dipole-like, having diverse polarization antennas (antenna with dual-linear polarization or circular polarization) help increase the tag detection reliability. Assets by itself can be dense or densely packed, and in these situations, the RF fields must be strong enough to excite tags after the attenuation caused by the dense assets and packages. Tag shadowing is yet another problem that causes misreads and decreases the accuracy/ Tag shadowing can be addressed by creating spatial diverse RF fields. Spatial diversity is created when RF fields emitted from two orthogonal axes (from both vertical and horizontal planes).

Traditional commercial antennas such as [2] are most commonly used to create standalone portals. These portals are often circularly polarized to offer polarization diversity but lack spatial diversity unless more than one antenna is used in different planes. Similarly, the standalone industrial portal [3] has multi-linear antennas to create polarization diversity only from the sides. Traditional portal antennas are often bulky and may not aesthetically fit in all applications. The proposed antenna is only 100 mm wide and thus fits both standard office doorframes and industrial doors. These commercial antennas [4 and 5] are narrow antennas but are only linearly polarized, thus does not meet the diversity requirements. The combo antenna configuration in [6] includes a vertically polarized side antenna, a horizontally polarized side antenna and a dual-linearly polarized top antenna. Although this antenna combo appears to create both spatial and polarization diversity, the combination fails when one half of the antenna is obstructed. For instance, when a person is obstructing the vertically polarized side antenna, the combination suffers from lack of vertically polarized fields.

This paper proposes a novel 'right-angled' 'V'- shaped UHF RFID reader antenna design that creates both polarization & spatial diversity that is compatible with any UHF RFID readers. A secondary antenna is not required at all to meet the diversity requirements. The antenna is conformal and can fit standard doorframes. The antenna is manufactured from a lightweight, non-toxic, low-cost, fire and chemical resistant substrate, making it comply with building codes and standards [7]. It is designed to fit the doorway/portal's corners. The 'V'- shaped antenna creates vertical and horizontally polarized fields at near-zone and creates a slant-polarized field at far-field distances. The antenna's beam is also steered to focus the RF energy on the intended scanning region.

Submitted on 02 March 2021. Dr. Prabakar Parthiban is with Times-7 Research Ltd, Lower Hutt, Wellington - 5010, New Zealand (e-mail: prabakarparthiban@gmail.com).

II. Related Works

This section elaborates on the uniqueness of the proposed antenna by comparing with other state-of-the-art designs in the literature. There are a lot of 'V'- shaped or 'L'- shaped patch antenna designs reported such as [8-12] which are less relevant to compare with the proposed antenna. This is because they talk about the two-dimensional shape of the patch antenna (which is 'V' like) instead of the proposed three-dimensional 'V'- shaped patch antenna array. A 2-Dimensional shaped patch refers to the patch geometry itself. For example, a rectangular patch or a circular patch refers to the 2-Dimensional geometry of the patch. There are only a few 3-Dimensional bent patch antenna array designs found in the literature for comparison.

The patch antenna design shown in [13] is probably the most relevant comparable design. Bandwidth enhancement of the patch antenna is proposed in this paper by designing a bent single patch antenna. The patch is bent 90° to form a 'V'- shape in its center and has flat flaps on either side. The antenna's ground plane is flat, and the antenna is excited through an 'H' shaped coupling slot. Similarly, an array antenna is designed by having two folded 'V'- shaped patches and two 'H'- shaped coupling slots with a microstrip line feed network on a flat ground plane. The proposed patch antenna array is different because the whole array is bent 90°, including the ground plane instead of folding the patch alone. Patches remain flat, and the microstrip line feeding the patch is folded 90°. Patches are quarter wavelength long with a grounding strip at the edge, unlike half-wavelength patches used in [13]. The array's azimuth beam is tilted 30° to enhance the UHF RFID performance in 865 – 868 MHz range whereas the antenna design in [13] is usable only in 2 GHz. [13] does not have polarization and spatial diversity like the proposed antenna, which is critical in doorway/portal applications.

A wedge-shaped air substrate patch antenna is proposed in [14] where the edge-fed patch is angled 30° from the ground plane. The patch is microstrip line fed, and it is flat with no bends, unlike the proposed antenna. The radiator is a half-wavelength resonant leaf-shaped patch. The leaf-shaped antenna works for a wide range of frequencies from 3.05 GHz to 26.87 GHz. The proposed patch uses a non-conventional substrate that has several advantages such as chemical resistance, flame retardancy, high compression strength and so on, whereas the patch antenna used in [14] uses air as the dielectric substrate. Antennas with air substrate cannot handle light impacts or knock like the foamed PVC substrate, and the antenna is prone to damage. The leaf-shaped antenna is only linearly polarized in both near and far-zone, but the proposed antenna is multi-linearly polarized at near-zones and slant 45° polarized at far-zone.

The circularly polarized 'V' - shaped patch antenna described in [15] is similar to the single patch antenna described in [13] except for the presence of flat flaps on either side of the patch. Although this probe-fed antenna resonates between 826 and 1030 MHz, the actual usable frequency range that has 3 dB axial ratio is from 879 to 919. This frequency range is not suitable for RAIN RFID as this range does not cover either of the two major frequency spans used are 865 to 868 MHz (in Europe) and 902 to 928 (in the Americas). The proposed antenna is designed to work for the European RFID frequencies 865 - 868 MHz. The 6° beam tilt obtained by [15] is unintended, and it is a consequence of the asymmetric bend. The proposed antenna is designed with 30° beam tilt to focus the radiation within the portal and increase the read accuracy. Spatial and polarization diversity is lacking in [15].

An RFID tag antenna design with 'V' bend is reported in [16]. The design is similar to [15] and the single patch antenna design discussed in [13]. It is a single patch antenna which is inset-fed by a microstrip line and the patch surfaces on either side of the inset feed is termed as sub-patch. The tag antenna is intended to go on a corner of a carton (with a bent ground plane) so that the antenna can experience spatial diversity – can radiate from two planes. Although the antenna is spatially diverse, this sub-patch configuration is very different from the proposed dual-patch antenna array configuration. The proposed array antenna is right-angled to converge and combine the fields and does not produce diverging fields, as reported in [16]. Diverging fields refer to the patch element residing on the exterior of the bend as opposed to the interior. The near-zone and far-zone polarization are diverse as well, in the proposed antenna. The RFID tag antenna is designed for 2.45 GHz, and it is not suitable for use with UHF RFID readers as a reader antenna. The proposed antenna's radiation pattern is directional and focused with a 30° tilt angle while the tag antenna creates an omnidirectional field equivalent.

The antenna design in [17] is a circularly polarized patch antenna made from a 3D-printed concave substrate that focuses on the beam compared to a normal flat substrate and can be used in space-constrained UHF RFID applications due to its sleek design. Although the antenna can be installed in a wider doorway (150 mm), this antenna's gain is far less than the proposed antenna, and thus it is not suitable for the intended application. Moreover, the antenna needs a protective radome that will make the antenna bulky and stick out into the passage, becoming a hazard. There is no spatial or polarization diversity offered by this antenna either, unlike the proposed antenna.

III. Antenna Design and Fabrication

The antenna array design features two radiating patches that are corporate fed by two parallel microstrip lines. A 6 mm thick foamed PVC substrate is used to construct the patch antenna array. Foamed PVC has several advantages viz.; it is non-toxic, chemical resistant, flame retardant, has low moisture absorption and has high compression strength, to comply with building codes and standards. Tinned steel sheet (0.2 mm thickness) is used as the array's ground plane. The ground plane and the radiating array are single parts whereas the substrate is two-part, spanning 205 mm x 100 mm each. The ground plane's dimensions are 416 mm x 100 mm, slightly (6 mm) longer than the joint length of the substrates (see Fig.1 (a)). Patches are quarter-wavelength long (70 mm), and its edges are shorted

with the ground plane by conductive copper tapes, like a planar inverted F-antenna (PIFA). A half-wavelength patch will be 140 mm long and would not fit the width of the doorway. Thus, a shorted patch design is opted to conform with the environment. Width of the patches is 154 mm, each. The patch antenna's length and width are calculated to operate at European RFID frequencies (commonly known as ETSI band), 865 to 868 MHz with fc being 866.5 MHz.

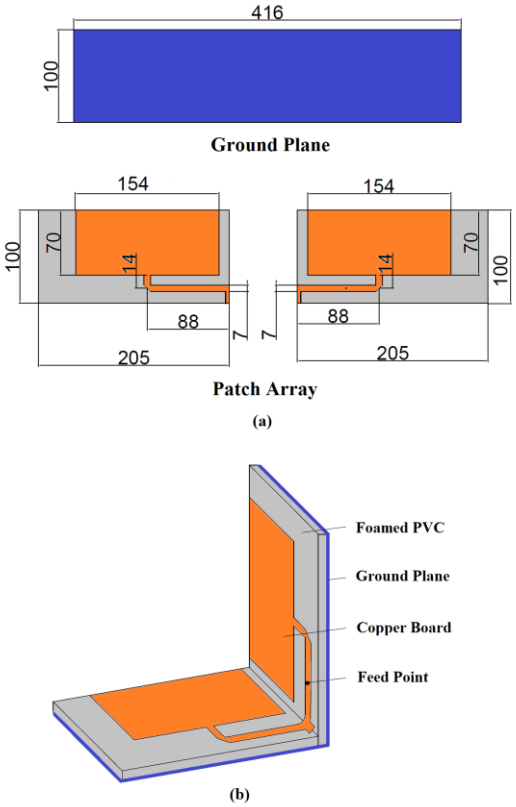

Fig. 1. Proposed antenna design: (a) 2-D view and (b) 3-D view

Patches are edge-fed by 100 Ω microstrip lines, which is a resultant of the impedance split from the 50 Ω input. Microstrip lines are 88 mm long and 10 mm wide. Although the edge impedance of the patch is slightly higher (128 Ω), an intentional impedance mismatch is made to increase the antenna's return loss bandwidth [18]. This small percentage of impedance mismatch does not affect the antenna's efficiency significantly. The input feed is offset by 50 mm to create a phase difference between the patches and to steer the antenna's beam to the left by 30°. The antenna's microstrip line is stub tuned to improve its impedance matching. The stub is 10 mm x 10 mm, refer Fig.1. Two substrate layers are adhered to the ground plane with a 6 mm gap in between, using an acrylic adhesive. One side of the substrate is folded 90° to obtain a right-angled 'V'-shaped patch antenna (refer Fig. 1 (b)). The radiating element array is then adhered to the substrate using the same acrylic adhesive. Patches are 12 mm apart and are orthogonal to each other. Copper foil tapes with conductive adhesive are used to short the edge of the patch antenna with the ground plane. A rear mount 50 Ω SMA connector is attached by soldering the center pin with the feed network and the ground with the antenna's ground plane. Pictured of the fabricated antenna is shown in Fig. 2.

Rear connector is preferred as the coaxial cable can be routed seamlessly through the walls to the reader port. The antenna does not bear a radome currently, but when it is manufactured commercially, a protective radome is recommended to use. Copper foil grounding can be replaced by shorting pins/vias along the patches' edges to increase the manufacturing reliability. The antenna's performance is not affected by a thin film of acrylic paint coating. It has been experimented with black paint to make it conformal with a black colored office door frame, used for test purposes. Fig. 3 (a) and (b) shows the painted antenna that conforms with black colored doorframe (Fig. 3(C)) when corner mounted.

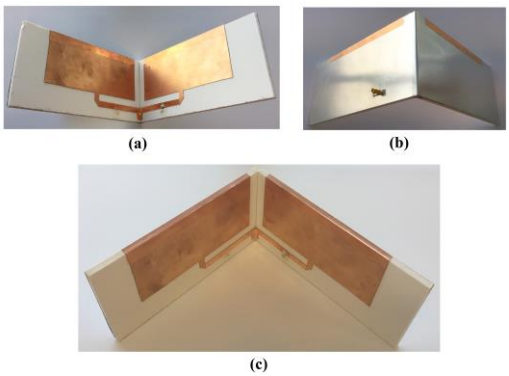

Fig. 2. Fabricated antenna: (a) Front view, (b) Rear view and (c) 3-D view

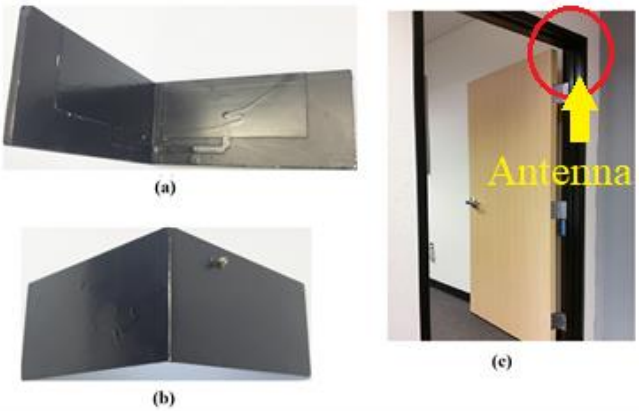

Fig. 3. Painted radomeless antenna: (a) Front view, (b) Rear view and (c) test doorway/portal

IV. Measurements

TR/1300 VNA (Vector Network Analyzer) is used to measure the antenna's return loss and gain performance in an anechoic chamber. The antenna's gain is measured by the comparison method using a calibrated reference antenna. The reference antenna is a linearly polarized Yagi-Uda antenna. The antenna's orientation is rotated between vertical, horizontal, slant 45° and negative slant 45° to measure differently polarized components radiated by the right-angled 'V'-shaped antenna.

This article has been accepted for publication in a future issue of this journal, but has not been fully edited. Content may change prior to final publication. Citation information: DOI 10.1109/JRFID.2021.3076805, IEEE Journal of Radio Frequency Identification

The antenna resonates efficiently at ETSI band with 18 dB return loss at fc. Fig. 4 shows the measured and 3D-EM simulated (EM Pro) plots. Although the operating band is only 4 MHz wide, the antenna's -10 dB bandwidth potential is 38 MHz. The return loss plot has a dip at 872 MHz, and this should not be confused as the antenna's resonant frequency. The antenna's radiation parameters confirm that the antenna is efficient at 866.5 MHz, thus resonant at the same frequency. Wideband antenna designs commonly have equal ability to radiate efficiently in frequencies below and above the dip.

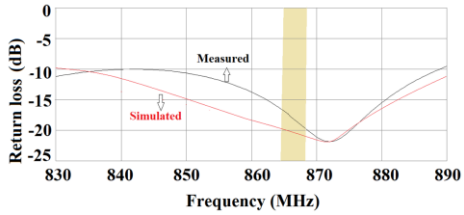

Fig. 4. Measured and simulated return loss plots

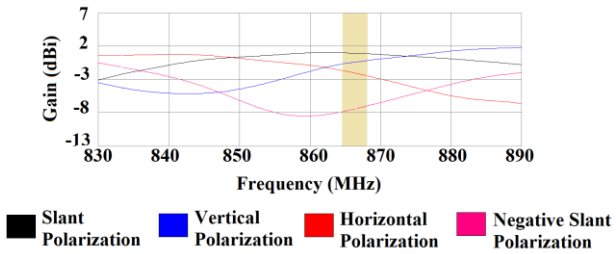

Fig. 5. Gain measured by orienting the left patch's boresight to the receiver.

The antenna's gain is measured in three orientations for four different polarizations to understand it's in spatial and polarization efficiency, viz., a) gain measured by orienting the left patch's boresight to the receiving antenna, b) gain measured by orienting the right patch's boresight to receiving antenna, c) gain measured by orienting the antenna's 'V'-boresight to the receiving antenna. Fig. 5 and Fig. 6 shows gain measurements of the left and right patch, respectively. Fig .7 shows the gain measurements of the 'V'-boresight. It is noted that the antenna radiates well in all four polarizations in the first two cases whereas the antenna's radiation is very efficient in slant polarization, in the final case. There is only about 10 dB gain difference between the slant and negative slant polarization in the first two cases, whereas the difference is more than 15 dBi in the final case. The fc measurement for various test antenna orientations and polarization are listed in Table. I. 3D-simulated beam pattern along with surface current distribution at different phases is also included to understand the antenna's radiation (see Fig. 9). At 0° phase the left patch did not get enough energy and at 30° phase the signal reaches to resonate both patches.

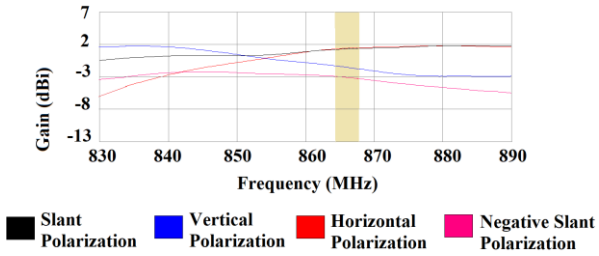

Fig. 6. Gain measured by orienting the right patch's boresight to the receiver

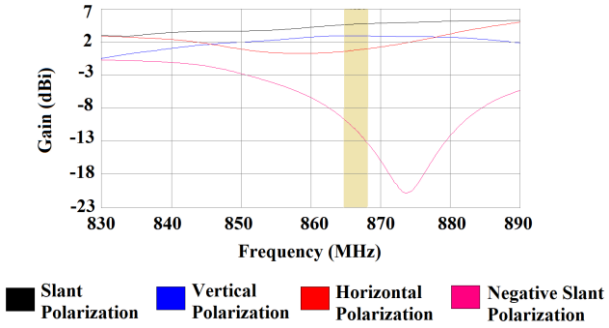

Fig. 7. Gain measured by orienting the antenna's 'V'- boresight to the receiver.

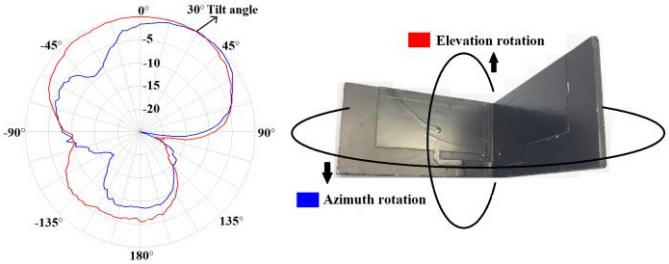

Fig. 8. Far-field patterns measured using the slant 45° polarized receiver (left) and Antenna's measurement orientation (right).

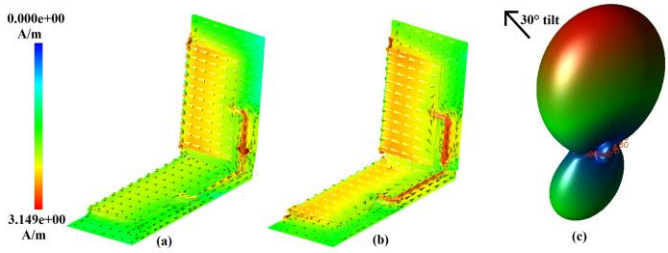

Fig. 9. Simulated surface current distribution: (a) at 0° Phase , (b) at 30° Phase and (c): 3D far-field pattern showing the beam tilt

TABLE I. MEASUREMENTS AT 866.5 MHZ ETSI CENTER FREQUENCY

Parameter at 866.5 MHz	Left patch Gain	Right patch Gain	'V' shaped Gain
Vertical polarized gain	0 dBi	-1.8 dBi	3 dBi
Horizontal polarized gain	-2 dBi	1.2 dBi	0.9 dBi
Slant polarized gain	1.2 dBi	1.2 dBi	5.5 dBi
Negative slant polarized gain	-8.2 dBi	-3 dBi	-11.2 dBi

This article has been accepted for publication in a future issue of this journal, but has not been fully edited. Content may change prior to final publication. Citation information: DOI 10.1109/JRFID.2021.3076805, IEEE Journal of Radio Frequency Identification

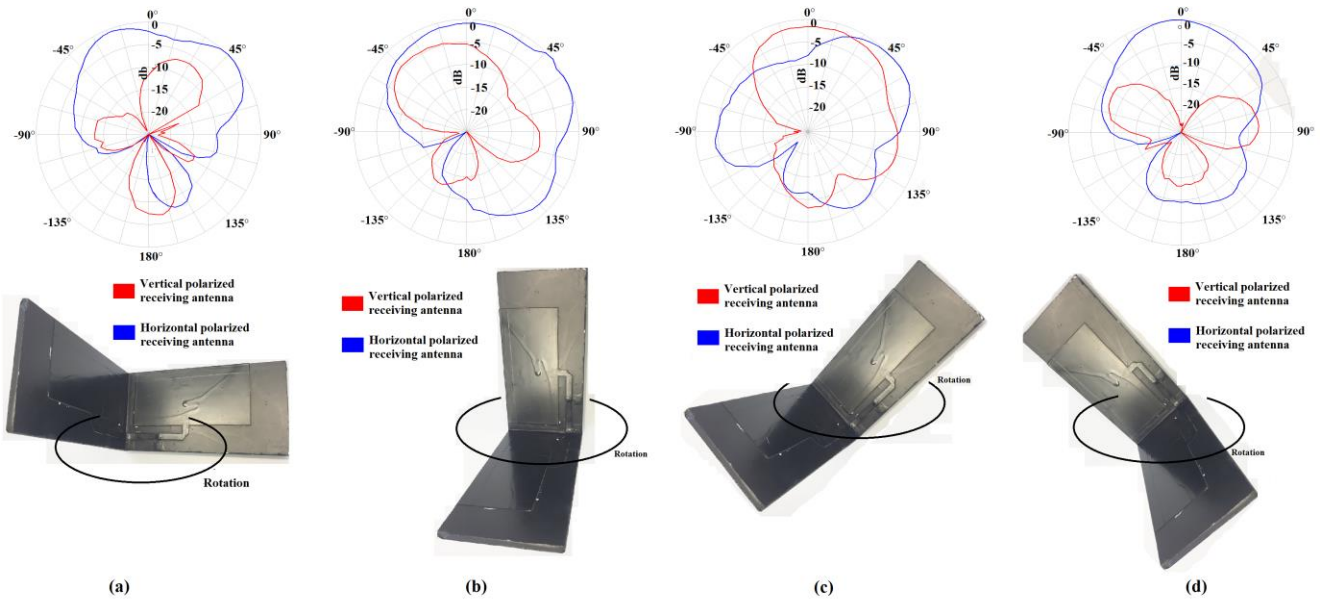

Fig. 10. Radiation pattern measured using vertical and horizontal polarized receiving antennas – (a) antenna at 0° rotation, (b) antenna at 90° rotation, (c) antenna at slant 45° rotation and antenna at slant 45° rotation

TABLE II. PROPOSED ANTENNA DESIGN VS EXISTING DESIGNS SUMMARY OF PERFORMANCE DIFFERENCES

Ref.	Near zone polarization	Far zone polarization	Array antenna?	V/ L shape	Antenna beam tilt?	Efficient operating frequency range	Polarization diversity	Spatial diversity
[8-12]	Not specified	Linear	No, Single patch antennas	No. Patch's shape itself is V/L - like	No beam tilt exists	X-band (8-12 GHz), 2-6 GHz and 60 GHz	Not diverse	Not diverse
[13]	Not specified	Vertical Linear	Dual-patch array	Each patch is bent to V shape on a flat ground plane	No beam tilt exists	1.65 to 2.2 GHz	Not diverse	Not diverse
[14]	Not specified	Vertical Linear	No, single patch	Wedge shaped slant single patch	No beam tilt exists.	3.05 GHz to 26.87 GHz	Not diverse	Not diverse
[15]	Not specified	Circular	No, single patch	Yes, single patch is bent to form V/L	Unintended 6° tilt due to asymmetry	Part of UHF RFID frequencies (879 – 919 MHz)	Not diverse	Not diverse
[16]	Not specified	Vertical Linear	No, Single patch	Yes, single patch is bent to form V/L	No beam tilt exists	2.45 GHz RFID frequency	Not diverse	Yes, radiation from two planes
[17]	Not specified	Circular	No, Single patch	No, a concave shaped substrate	No beam tilt exists	UHF RFID frequencies (865 – 868 MHz)	Not diverse	Not diverse
This work	Multi-linear polarization	Slant 45° linear	Yes, dual patch array	Yes, array is right-angled including the ground plane	Yes, 30° beam tilt	UHF RFID frequencies (865 – 868 MHz)	Yes, Multi-linear and Slant 45°	Yes, radiation from two planes

V. Analysis

Table II shows the performance differences between the proposed right-angled 'V'- shaped antenna design and existing 'V' or 'L' – shaped designs. It is clear that the proposed design meets all the requirement for an efficient doorway/portal application viz., polarization and spatial diversity, beam tilt to focus the radiation, physically slim and conformal to the doorway, rugged and robust to handle minor impacts and knocks. In addition to the slant polarized radiation pattern reported in Fig. 8, horizontal and vertically polarized radiation patterns are also measured for four different antenna orientations viz., 0°, 90°, slant 45° and negative slant 45°. These measurements help us to visualize the RF field spread experienced by RFID tags traveling across the doorway/portal in different orientations. Fig. 10 shows that horizontally polarized fields are dominant at 0°, 90° and slant 45° orientations. Vertically polarized fields are dominant in 45° orientation and, ~5 dB and ~10 dB less dominant in 90° and 0° orientations, respectively.

As the antenna is slant 45° polarized, the orthogonal negative slant polarization (i.e., the vertical polarization in Fig. 10(d)) is almost null. Similarly, the horizontally polarized pattern seen in Fig. 10(c) is the orthogonal negative slant 45° polarization of the slant 45° polarization (vertical polarization); thus, it is ~7 dB less dominant. It is worth mentioning that patterns measured are a combination of azimuth and elevation. For instance, the horizontally polarized elevation pattern of the antenna orientation shown in Fig. 10(a) is the vertical polarized pattern shown in Fig. 10(b). This applies to all different antenna orientations. The horizontal polarization may be dominant in Fig. 11, but in fact, some of the horizontally polarized patterns are vertically polarized patterns of the antenna's elevation plane. The antenna is tested for RAIN RFID doorway/portal application. The antenna is mounted on a 1' wide x 6' tall doorway (at the corner) and a single RFID tag' RSSI (Return Signal Strength Indicator) is noted by moving the tag within the doorway. The doorway is virtually segmented to obtain 45 test points, as shown in Fig. 11. Impinj R420 RAIN RFID reader [19] is used along with Smartrac dogbone Monza r6 tag [20] is used for testing. The tag is held using a polystyrene rod during the test process to avoid human attenuation. The doorframe is not real, but a timber frame placed on a concrete floor is used.

The antenna is connected to the Impinj reader with a 2-meter RG-58 cable (~1 dB cable loss) and operated at 30 dBm output power. Impinj reader mode '1000: Autoset dense reader' is chosen along with 'session 1' and 'dual-target' search mode. Two RSSI profiles are recorded for vertical (along the 6' doorway length) and horizontal tag (along the 3' doorway width) orientations. Recorded values are plotted as a heat map to visualize the RF field strength from the RFID tag's perspective (see Fig. 12). From this testing, it is vivid that the proposed right-angled 'V' - shaped antenna is robust enough to tags traversing through doorway/portal in different orientations with its polarization and spatial diversity. The field intensity is lower at the top-left and bottom-right corners of the doorway/portal and higher along the diagonal (along the direction of propagation but slightly down tilted). If there is a requirement to have high-intensity signals at the top-left and bottom-right corners, a secondary antenna can be added on the top-left corner of the doorway/portal.

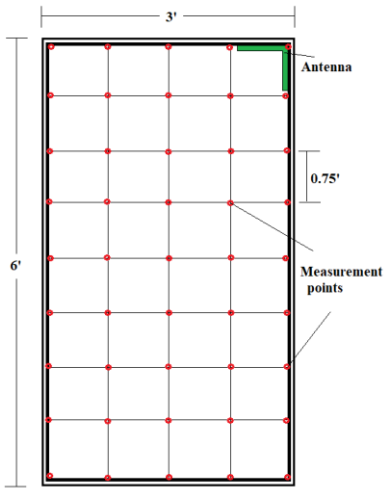

Fig. 11. RFID test measurement setup

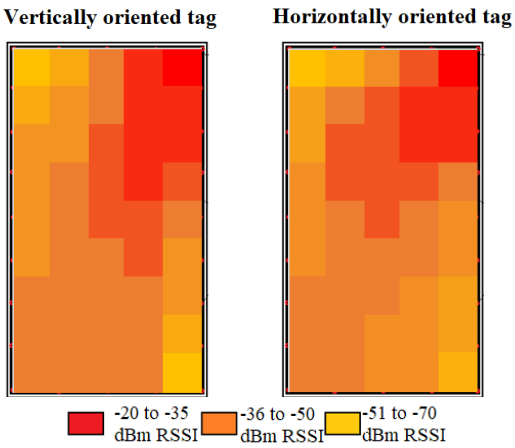

Fig. 12. RSSI measurements of the test tag

As per Fig. 9(c) and Fig. 10, the antenna's beam will be oriented to create a wider radiation in-and-out of the doorway. These figures are normalized radiation patterns and do not provide absolute measurements in measurement-units. RFID radiation boundary measurement using an RFID tag and a reader is essential to visualize the RF fields for a robust RFID deployment. Thus, the radiation in both planes (elevation and azimuth) is measured in millimeters using a single Smartrac dog-bone RFID tag at the antenna's boresight. A slotted tag board is created using a medium-density fiber (MDF) board that is 1220 x 2440 mm (See Fig. 13). Slots are spaced 100 mm apart, and there were 276 measurement points. Fig. 13 also shows the antenna's location (measuring the elevation plane), and it is rotated 90° for azimuth measurements. To be practical

about measuring the boundary and avoiding inconclusive results due to the environmental reflections, the antenna was operated at 10 dBm power. The tag's RSSI filter was set to maximum (-80 dBm). Only the anterior and lateral sides of the antenna were measured, and posterior measurements are omitted as it is not necessary in this use case. The test location was preferred to be an office or workspace to mimic the practical application environment. Tag is moved between slots to record tag detection, and the RFID radiation boundary is mapped for 14.5 dBm EIRP (effective isotropic radiated power). The antenna's transmit power (10 dBm), cable loss (1 dB), and antenna's gain (5.5 dBi) are used to calculate the EIRP. Fig. 14 (a) and (b) show the antenna's radiation boundary when oriented longways and sideways, respectively. These measurements are analogous to the antenna's wide and narrow radiation pattern shown in Fig. 8. Yet, plots are not smooth, unlike radiation patterns (Fig. 8), because of multipath reflections and coarse measurement intervals (100 mm grid spacing). The blue-colored area represents tag detection, while the green-colored area is just a background. Isolation between detecting intended and unintended tags can be easily obtained by moving the unwanted assets away from the RFID radiation boundary.

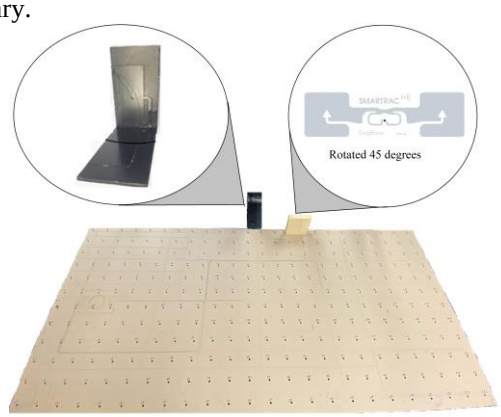

Fig. 13. Test Setup - Slotted MDF board with 276 measurement points with the Test tag and antenna oriented in the elevation plane.

VI. Real-life Testing

An RFID tag in free space is used in the previous section to evaluate and analyze the antenna's RFID read range and radiation pattern. In reality, tags will be attached to assets and they will be tracked as a group. Thus, it is important to test and verify the RFID system's performance with this novel antenna using various kinds of assets in large quantities. Challenges such as tag shadowing, tag detuning effect due to asset's density, etc., are examined in this section. In this paper, only retail assets are focused as doorway antennas are likely to be used in offices, clothing stores, stationery shops and so on, and not in other industry segments such as warehousing or healthcare. Three types of boxed assets are prepared, viz, 1) densely packed fabric assets, 2) sparsely packed stationery and household goods 3) a pack of 100 plastic balls. Different tag types were used for different assets, as tag manufacturers often prescribe the recommended tag for various goods

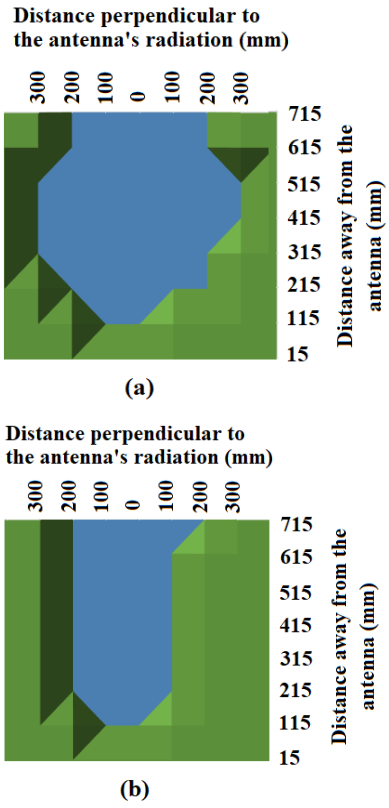

Fig. 14. RFID radiation boundary at 10 dBm for slant tag orientation (a) elevation plane and (b) azimuth plane.

.

1) Densely packed fabric assets

Regular fabric assets such as tea towels, cloth napkins, T-shirts, leggings, undies, etc., (See Fig.15(a)) are tagged using a Checkpoint Vortex tag. They are recommended for retail apparel tracking and they have adhered to the paper-based price tag (refer Fig. 15(c)). These are 31 tagged fabrics with unique electronic product codes (EPC) that are packed into a box that spans 290 x 290 x 50 mm. A Vortex tag is stuck on the outside of the box too. This is a standard practice in the RFID industry to enable box-level and item-level tracking. On the whole, there are 32 tags that to be tracked. These fabrics are tightly packed with no spacers in between in a small box. Price tags were folded into the fabric, and they are not oriented in the same manner.

Fig. 15. (a) Fabric assets and (b) Densely packed in a box (c) Checkpoint Vortex Tag.

2) Sparsely packed stationery and household goods

Goods include pouches, hard-bound books, silicone molds, other plastic kitchen items, etc., are sparsely packed with foam cushions in between. There are a total of 20 items in a 500 x 200 x 170 mm sized carton. In the retail industry, goods are either individually packed or packed with foam cushions or spacers as they are often fragile. Smartrac mini-web tag is used on these assets, and they are randomly oriented inside the box. There is no tag on the outside of the box.

(a) (b) (c)

Fig. 16. (a) Stationary assets, (b) Sparsely packed in a box, and (c) Smartrac Mini-Web Tag.

3) A pack of 100 plastic balls

A pack of 100 plastic balls is individually tagged and tested to simulate a different type of densely packed assets where tags are curled and intentionally shadowed. Avery Dennison's AD-237 R6P tag is used for this use case. These assets won't bear an outside tag too. AD-237 R6P tag is far more sensitive than the Vortex tag.

(a) (b)

Fig. 17. (a) A pack of 100 plastic balls and (b) Avery Dennison AD-237 Tag

The antenna is mounted on the right-hand top corner of a single doorway. Assets are traversed by hand-carrying them (refer Fig. 18(a)) to include human interference and by pushing them through an open cart with no metal-bound as shown in Fig. 18(b). For a thorough test, all three cartons are rotated each time so that each of the six faces of the carton is pointed towards the top of the doorframe. Six faces are marked from A to F, as shown in Fig. 19. The antenna is operated at 30 dBm at all times with the default reader settings similar to the one mentioned in section V. The antenna creates a larger read window due to its wider beamwidth in the elevation plane.

Table III and Table IV show the test results for both scenarios – hand-carried assets and assets moved through the cart. Hand-carried assets are a little harder to read, especially the dense fabric assets with slightly insensitive tag. Th

e densely packed plastic balls are able to be read consistently as they had sensitive tags. In certain faces, the outside tag was directly covered by hands in the fabric asset box and thus, the read accuracy is affected. At Face-D, the maximum and minimum RSSI is noted to be -80.5 dBm and -75.5 dBm. The energy penetration through Face-D is the hardest compared to other faces. On the other hand, when these assets are carried on the cart, they were able to be read comfortably. This shows that human body attenuation makes it harder to detect tags efficiently. TO overcome this problem, as suggested in section V, it is wise to add one more antenna on the other side of the doorway to increase the probability of detection.

(a) (b)

Fig. 18. (a) Hand-carried scenario (b) An open cart used for the testing

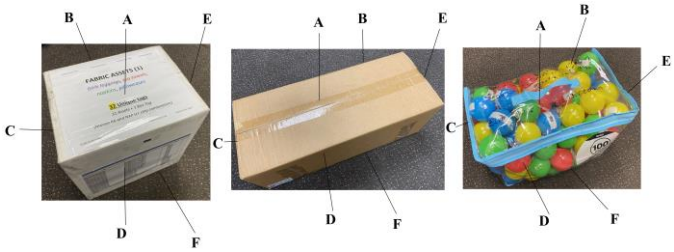

Fig. 19. A to F, Six faces in each asset. A: top face, B: side 1, C: side 2, D: side 3, E: side 4, and F: bottom face.

TABLE III. HAND CARRIED ASSETS

Face	Asset type	Detection accuracy %	Min/Max RSSI (dBm)	Speed of detection (seconds)
A	Densely packed fabric	100	-58.5/-70.5	8
	Sparsely packed goods	100	-55.0/-58.5	5
	Pack of 100 plastic balls	100	-53.5/-59.0	10
B	Densely packed fabric	96.87	-62.5/-76.5	8
	Sparsely packed goods	100	-49.0/-52.5	5
	Pack of 100 plastic balls	100	-55.5/-62.0	10
C	Densely packed fabric	96.87	-61.5/-77.0	8
	Sparsely packed goods	100	-51.5/-53.5	5
	Pack of 100 plastic balls	100	-54.5/-63.5	11
D	Densely packed fabric	93.75	-75.5/-80.5	8
	Sparsely packed goods	100	-48.0/-55.5	5
	Pack of 100 plastic balls	100	-57.5/-64.0	10
E	Densely packed fabric	96.87	-68.5/-71.5	8
	Sparsely packed goods	100	-50.5/-57.5	5
	Pack of 100 plastic balls	100	-55.5/-61.50	11
F	Densely packed fabric	100	-54.5/-69.5	9
	Sparsely packed goods	100	-55.0/-57.5	4
	Pack of 100 plastic balls	100	-57.5/-59.0	9

TABLE IV. ASSETS MOVED THROUGH THE CART

Face	Asset type	Detection accuracy %	Min/Max RSSI (dBm)	Speed of detection (seconds)
A	Densely packed fabric	100	-54.5/-68.5	7
	Sparsely packed goods	100	-37.5/-47.0	5
	Pack of 100 plastic balls	100	-39.5/-51.0	6
B	Densely packed fabric	100	-52.5/-69.5	8
	Sparsely packed goods	100	-41.5/-48.0	6
	Pack of 100 plastic balls	100	-41.5/-52.0	8
C	Densely packed fabric	100	-49.5/-62.5	8
	Sparsely packed goods	100	-41.5/-47.0	5
	Pack of 100 plastic balls	100	-46.5/-56.0	6
D	Densely packed fabric	100	-54.5/-68.5	8
	Sparsely packed goods	100	-46.5/-57.0	6
	Pack of 100 plastic balls	100	-47.5/-51.0	5
E	Densely packed fabric	100	-54.5/-68.5	6
	Sparsely packed goods	100	-39.5/-51.5	5
	Pack of 100 plastic balls	100	-46.5/-53.5	6
F	Densely packed fabric	100	-55.5/-67.5	8
	Sparsely packed goods	100	-43.5/-55.0	4
	Pack of 100 plastic balls	100	-49.5/-59.0	6

VII. CONCLUSION

A novel right-angled ‘V’-shaped RAIN RFID reader antenna is designed, fabricated and analyzed for doorway/portal applications. The antenna is conformal; it is seamless when installed on a doorway/portal. The antenna’s polarization and spatial diversity help to detect tags in various tag orientations and in different planes. The antenna’s radiation characteristics are analyzed in different planes, and the same is confirmed using comprehensive RFID tag testing. Real-life asset tests are performed to evaluate the antenna’s performance in practice. The antenna’s beam tilt helps to focus the radiation in the intended read zone. As part of future work, a right-angled ‘V’ -shaped antenna will be designed and tested for FCC RAIN RFID frequencies, 902 to 928 MHz.

ACKNOWLEDGMENT

Dr. Parthiban would like to thank Times-7 Research Ltd for their support and encouragement towards his Ph.D. completion at the Auckland University of Technology, New Zealand.

REFERENCES

[1] RAIN RFID (2020, January 21). RAIN RFID [Online]. Available: https://rainrfid.org/

[2] Laird S9028PCR/PCL (2020, January 21). Laird tech [Online]. Available: https://assets.lairdtech.com/home/brandworld/files/ANT-DS-S9028PCL%20S9028PCR-0515.pdf

[3] SLS portal complete (2020, January 21). SLS [Online]. Available: https://www.slsrfid.com/product/smartportal-complete/

[4] Threshold (2020, January 21). Impinj [Online]. Available: https://www.impinj.com/platform/connectivity/threshold/

[5] A8060 (2020, January 21). Times-7 [Online]. Available: https://www.times-7.com/a8060-door-frame-antenna-(lp).html

[6] A8065 combo (2020, January 21). Times-7 [Online]. Available: https://www.times-7.com/slimline-a8065-combo-doorway-portal-solution.html

[7] P. Parthiban, "Fixed UHF RFID Reader Antenna Design for Practical Applications: A Guide for Antenna Engineers With Examples," International Journal on Smart Sensing and Intelligent Systems, vol. 12, no. 1, pp. 1-8, Sept. 2019.

[8] P. Borah and S. Bhattacharyya, "Design of a fan beam 1×4 array antenna using V-shaped patch element for its use in X-band communication," 2019 URSI Asia-Pacific Radio Science Conference (AP-RASC), New Delhi, India, 2019, pp. 1-4.

[9] S. R. Rama and D. Vakula, "Triangular patch antenna with asymmetric V-slots for tri-band wireless applications," 2014 IEEE International Microwave and RF Conference (IMaRC), Bangalore, 2014, pp. 293-296.

[10] H. Elsadek and D. M. Nashaat, "Multiband and UWB V-Shaped Antenna Configuration for Wireless Communications Applications," IEEE Antennas and Wireless Propagation Letters, vol. 7, pp. 89-91, 2008.

[11] M. F. Haider, S. Alam and M. H. Sagor, "V-Shaped Patch Antenna for 60 GHz mmWave Communications," 2018 3rd International Conference for Convergence in Technology (I2CT), Pune, 2018, pp. 1-4.

[12] J P. Borah, A.K. Bordoloi, N.S. Bhattacharyya and S. Bhattacharyya, “Bridged ‘V’-shaped patch antenna for dualband communication” Electronic Letters, vol. 48, no. 8, April 2012.

[13] F. Dong, W. Lin, X. Guo, and G. Wang, “A Wide Bandwidth Folded V-Shaped Patch Antenna with Stable High Gain and Low Cross-Polarization Characteristics”, Progress in Electromagnetic Research -C, vol. 62, pp. 51-59, 2015.

[14] Feng-Wei Yao, Shun-Shi Zhong and Xian-Ling Liang, "Ultra-broadband patch antenna using a wedge-shaped air substrate," 2005 Asia-Pacific Microwave Conference Proceedings, Suzhou, 2005.

[15] Y. Pan, Y. Dong and Z. Wang, "Circularly Polarized V-Shaped Patch Antenna for RFID Application," 2019 IEEE International Symposium on Antennas and Propagation and USNC-URSI Radio Science Meeting, Atlanta, GA, USA, 2019, pp. 1893-1894.

[16] A. Rawal and N. C. Karmakar, "A novel L-shaped RFID tag antenna," 2007 European Microwave Conference, Munich, 2007, pp. 1003-1006.

[17] P. Parthiban, "3D-printed circularly polarized concave patch with enhanced bandwidth and radiation pattern," Microwave and Optical Technology Letters, vol. 63, Issue 2, pp. 572-580, 2021.

[18] P. Parthiban, " Bandwidth enhancement for thin substrate UHF RFID patch antenna," IEEE Journal of Radio Frequency Identification, vol. 3, no. 3, pp. 191-204, 2019.

[19] Speedway r420 (2020, January 22). Impinj [Online]. Available: https://www.impinj.com/platform/connectivity/speedway-r420/

[20] Dogbone Monza R6 (2020, January 22). Smartrac [Online]. Available: https://www.smartrac-group.com/dogbone.html

Dr. Prabakar Parthiban (S’16 – G’21) received the Bachelor of Electronics and Communications Engineering degree (first class) from Anna University, India in 2010 and the Master of Engineering Studies degree with Distinction from the Auckland University of Technology (AUT), New Zealand in 2012. He completed his Ph.D. Degree in electronics engineering (majoring in antennas and microwave) from AUT in December 2020. He is currently employed as the ‘Head of Engineering and RF Specialist’ at Times-7 Research Ltd, New Zealand. He has more than 9 years of industrial work experience in antenna design, testing and commercialization along with compliance and regulatory know-how. His current research interests are in IoT, RAIN RFID, and other Auto-ID technologies.